


Neuropilin-1 is required for endothelial cell adhesion to soluble vascular endothelial growth factor receptor 1

Gianni Colotti¹, Cristina Maria Failla², Pedro Miguel Lacal³, Mariangela Ungarelli⁴, Federica Ruffini³, Patrizio Di Micco^{5,*}, Angela Orecchia⁴ and Veronica Morea¹ 

1 Institute of Molecular Biology and Pathology (IBPM) of the National Research Council (CNR), Rome, Italy

2 Laboratory of Experimental Immunology, IDI-IRCCS, Rome, Italy

3 Laboratory of Molecular Oncology, IDI-IRCCS, Rome, Italy

4 Laboratory of Molecular and Cell Biology, IDI-IRCCS, Rome, Italy

5 Department of Biochemical Sciences 'A. Rossi Fanelli', Sapienza' University of Rome, Italy

Keywords

angiogenesis; neuropilin-1; peptides;
vascular endothelial growth factor receptor
1; $\alpha 5\beta 1$ integrin

Correspondence

V. Morea, Institute of Molecular Biology and Pathology (IBPM) of the National Research Council of Italy (CNR) c/o Department of Biochemical Sciences 'A. Rossi Fanelli', 'Sapienza' University, P. le Aldo Moro 5, 00185 Rome, Italy
Tel. +39 06 49910556
E-mail: veronica.morea@cnr.it

Present address

*Department of Data Science, The Institute of Cancer Research, London, UK

Gianni Colotti and Cristina Maria Failla contributed equally to this article

(Received 11 November 2019, revised 27 May 2021, accepted 12 July 2021)

doi:10.1111/febs.16119

Neuropilin-1 (NRP-1) is a semaphorin receptor involved in neuron guidance, and a co-receptor for selected isoforms of the vascular endothelial growth factor (VEGF) family. NRP-1 binding to several VEGF-A isoforms promotes growth factor interaction with VEGF receptor (VEGFR)-2, increasing receptor phosphorylation. Additionally, NRP-1 directly interacts with VEGFR-1, but this interaction competes with NRP-1 binding to VEGF-A165 and does not enhance VEGFR-1 activation. In this work, we investigated in detail the role of NRP-1 interaction with the soluble isoform of VEGFR-1 (sVEGFR-1) in angiogenesis. sVEGFR-1 acts both as a decoy receptor for VEGFs and as an extracellular matrix protein directly binding to $\alpha 5\beta 1$ integrin on endothelial cells. By combining cell adhesion assays and surface plasmon resonance experiments on purified proteins, we found that sVEGFR-1/NRP-1 interaction is required both for $\alpha 5\beta 1$ integrin binding to sVEGFR-1 and for endothelial cell adhesion to a sVEGFR-1-containing matrix. We also found that a previously reported anti-angiogenic peptide (Flt₂₋₁₁), which maps in the second VEGFR-1 Ig-like domain, specifically binds NRP-1 and inhibits NRP-1/sVEGFR-1 interaction, a process that likely contributes to its anti-angiogenic activity. In view of potential translational applications, we developed a five-residue-long peptide, derived from Flt₂₋₁₁, which has the same ability as the parent Flt₂₋₁₁ peptide to inhibit cell adhesion to, and migration towards, sVEGFR-1. Therefore, the Flt₂₋₅ peptide represents a potential anti-angiogenic compound *per se*, as well as an attractive lead for the development of novel angiogenesis inhibitors acting with a different mechanism with respect to currently used therapeutics, which interfere with VEGF-A165 binding.

Introduction

Neuropilin-1 (NRP-1) is a transmembrane protein involved in diverse cellular functions [1]. It is the receptor of different members of the semaphorin family implicated in axon guidance in neurons [2,3]; it acts

Abbreviations

3D, three-dimensional; ECs, endothelial cells; NIP, neuropilin-interacting protein; NRP, neuropilin; PDB, Protein Data Bank; RU, resonance units; SASA, solvent accessible surface area; shRNA, small hairpin RNA; SPR, surface plasmon resonance; sVEGFR-1, soluble VEGFR-1; tmVEGFR-1, transmembrane VEGFR-1; VEGF, vascular endothelial growth factor; VEGFR, VEGF receptor.

as a co-receptor for vascular endothelial growth factor (VEGF) family members in endothelial cells (ECs) [4,5], and it mediates cell adhesion to the extracellular matrix [6]. Moreover, it has been shown that NRP-1 stimulates growth of different tumour types [7–9], while NRP-1 silencing suppresses cancer cell growth [10]. Further, NRP-1 has been proposed to modulate immune cell activities in tumour immune surveillance [11]. Importantly, NRP-1 has been recently demonstrated to be a host factor for SARS-CoV-2 infection [12,13].

Neuropilin-1 structure comprises three regions: extracellular, membrane and cytoplasmic. The extracellular region, in turn, comprises five domains: (1) two complement-binding like domains (a1 and a2); (2) two coagulation factor V/VIII homology domains (b1 and b2); and (3) one MAM domain homologous to metalloendopeptidase mepripin, A5 and mu-phosphatase (c). Some of these regions have been associated with specific NRP-1 functions. The a1, a2 and b1 domains have been shown to be involved in class 3 semaphorin binding. The b1-b2 domains are implicated in both VEGF binding [14] and cell adhesion [1]. The role of the c domain is less clear. It was initially proposed to be involved in dimerization [2], based on cell experiments on NRP-1 deletion variants and in analogy with other MAM domains. This hypothesis was subsequently challenged by the results of isothermal titration calorimetry experiments on the purified MAM domain, which indicate that, even if homo-dimerization took place, the association constant would be weak [15]. Other roles proposed for this domain include the separation of the a1a2b1b2 domains from the membrane and their correct positioning for other intermolecular interactions [15]. The intracytoplasmic tail comprises ~40 amino acids and interacts with the neuropilin-interacting protein (NIP) [16].

Interaction with NRP-1 mediates, at least in part, cell signalling by growth factors belonging to the VEGF family, including VEGF-A isoforms VEGF-A165, VEGF-A189 and VEGF-A206 [17–19] but not VEGF-A145 [20]. When co-expressed with the VEGF receptor (VEGFR)-2, NRP-1 enhances VEGF-A165 binding to VEGFR-2 and VEGF-A165-mediated chemotaxis [5]. Additionally, NRP-1 functions as an enhancer of VEGF-A165-mediated mitogenic response in human ECs [21]. Consistent with NRP-1 role in modulating VEGF-A165 availability and functions, NRP-1 knock-out mice die at the embryo stage with defects in both the nervous and cardiovascular systems [22], whereas NRP-1 over expression causes anomalies at the cardiovascular level, such as excess capillaries and blood vessels, and abnormal heart [23].

Neuropilin-1 has additional effects on ECs, which are not exerted by interference with VEGF-A165 signalling. NRP-1 regulates EC adhesion to extracellular matrix proteins independent of VEGFR-2, as demonstrated by using RNA interference-mediated silencing of NRP-1 or VEGFR-2 in primary human ECs [21]. Moreover, neither class 3 semaphorins or VEGF-A165 interfere with NRP-1 action in cell adhesion [1]. NRP-1 also interacts with $\alpha 5\beta 1$ integrin at sites of EC adhesion to fibronectin [24] and with $\beta 1$ integrin subunit in tumour cells [25]. The interaction with $\alpha 5\beta 1$ integrin in ECs is mediated by the extracellular region, and regulation of $\alpha 5\beta 1$ integrin binding to fibronectin results from the interaction of the cytoplasmic tail with NIP and subsequent activation of integrin internalization and vesicle motility. On these bases, regulation of $\alpha 5\beta 1$ integrin trafficking was proposed to be one of the mechanisms by which NRP-1 exerts its role in angiogenesis [24].

Neuropilin-1 was also shown to directly and reversibly interact with VEGFR-1 [26,27]. This interaction competed with NRP-1 binding to VEGF-A165 and did not enhance VEGFR-1 activation or downstream signalling. The biological significance of this interaction is still unclear.

In addition to VEGFR-1 transmembrane form (tmVEGFR-1), soluble isoforms of the receptor are originated by alternative splicing of the same gene [28–30]. VEGFR-1 soluble isoform produced by ECs (sVEGFR-1) comprises the 656 N-terminal residues in the extracellular region (encompassing the first six immunoglobulin (Ig)-like domains), and a specific C-terminal sequence of 30 amino acids. sVEGFR-1 has a dual role in angiogenesis: (a) On the one hand, sVEGFR-1 binds VEGF-A165. This results in a reduced amount of VEGF-A165 available for VEGFR-2 binding and, therefore, in a downregulation of VEGFR-2-mediated angiogenic signalling. (b) On the other hand, sVEGFR-1 is deposited by ECs in the extracellular matrix. Here, sVEGFR-1 is involved in cell adhesion and migration via a direct interaction with $\alpha 5\beta 1$ integrin [31], through which it triggers molecular signals of motility and angiogenesis [32]. Moreover, sVEGFR-1/ $\beta 1$ integrin interaction has been demonstrated to be involved in the progression and response to anti-angiogenic therapies in squamous cell lung carcinoma [33].

With the goal to identify the sVEGFR-1 region interacting with $\alpha 5\beta 1$ integrin, we previously designed and tested twelve peptides, which cover almost entirely the surface of the second extracellular Ig-like domain of VEGFR-1 [34]. One of these peptides, comprising the 11 amino acid residue sequence NITVTLKKFPL

[34] had been previously reported with the name Flt₂₋₁₁ by a different group [35]. They found that Flt₂₋₁₁ had anti-angiogenic activity *in vivo*, but was not able to either bind VEGF-A165 or inhibit VEGF-A165 interaction with ECs [35]. Our subsequent studies showed that peptide Flt₂₋₁₁ (a) specifically inhibited EC adhesion to sVEGFR-1 but not to fibronectin [34]; (b) did not directly support $\alpha 5\beta 1$ integrin-mediated EC adhesion [34] and (c) inhibited EC migration towards sVEGFR-1 [36].

In the present work, we report that peptide Flt₂₋₁₁ binds to NRP-1 and inhibits NRP-1 interaction with sVEGFR-1. Hence, we take advantage of the peptide mechanism of action to elucidate the role of the NRP-1/sVEGFR-1 interaction in angiogenesis. Finally, we develop a five-residue derivative of peptide Flt₂₋₁₁ that has the same anti-angiogenic properties as the parent Flt₂₋₁₁.

These results expand our knowledge about NRP-1 role in angiogenesis and indicate that NRP-1 interaction with VEGFR-1 has a role in the modulation of EC adhesion to the extracellular matrix. Taken together, the discovery of a molecular mechanism involved in angiogenesis that is independent of VEGF-A165 binding, and of a short peptide able to inhibit this mechanism, opens the road to the development of novel anti-angiogenic therapies, both alternative and complementary to those targeting VEGF-A165 interactions.

Results

Flt₂₋₁₁ peptide binds to NRP-1 and specifically inhibits NRP-1 interaction with VEGFR-1

To elucidate the mechanism by which the anti-angiogenic Flt₂₋₁₁ peptide inhibits EC adhesion to, and migration towards, sVEGFR-1, we first investigated the peptide ability to bind known VEGFR-1 interactors. As shown in Fig. 1A, biotinylated Flt₂₋₁₁ peptide was able to bind NRP-1, whereas it did not bind to VEGFR-1 itself. Flt₂₋₁₁ peptide also bound neuropilin-2 (NRP-2), even though a direct interaction between NRP-2 and VEGFR-1 has not been previously demonstrated [37]. Additionally, Flt₂₋₁₁ peptide had been reported not to bind either VEGF-A165 or $\alpha 5\beta 1$ integrin [34,36].

NRP-1 binding by Flt₂₋₁₁ peptide was specific, since none of the four additionally tested peptides was able to bind either NRP-1 (Fig. 1B) or NRP-2 (data not shown). These four peptides were chosen because they all map on the surface of the second Ig-like domain of VEGFR-1 and are able to inhibit EC adhesion to sVEGFR-1 [34,36],

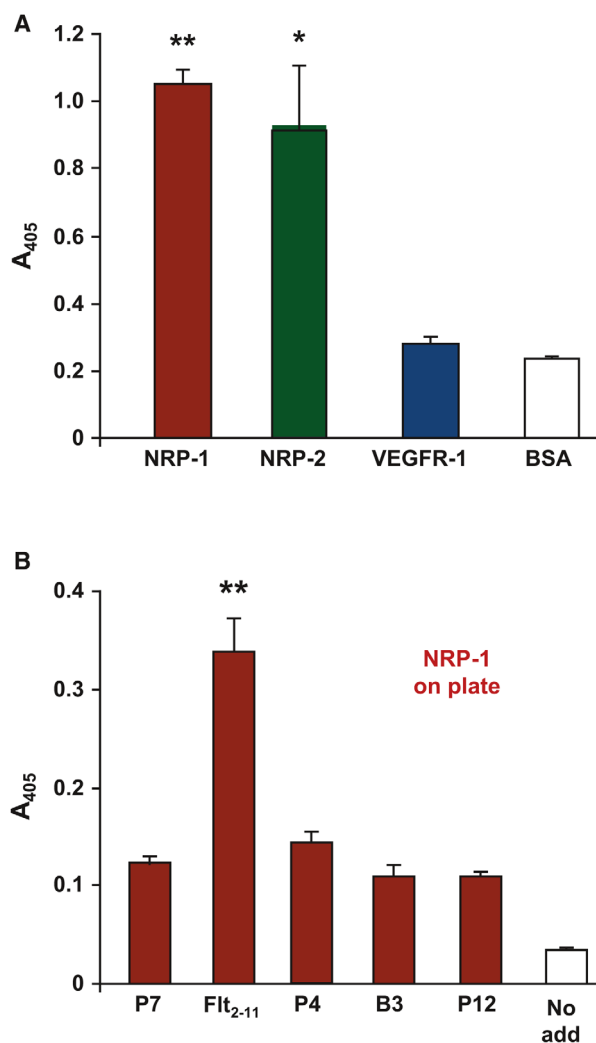
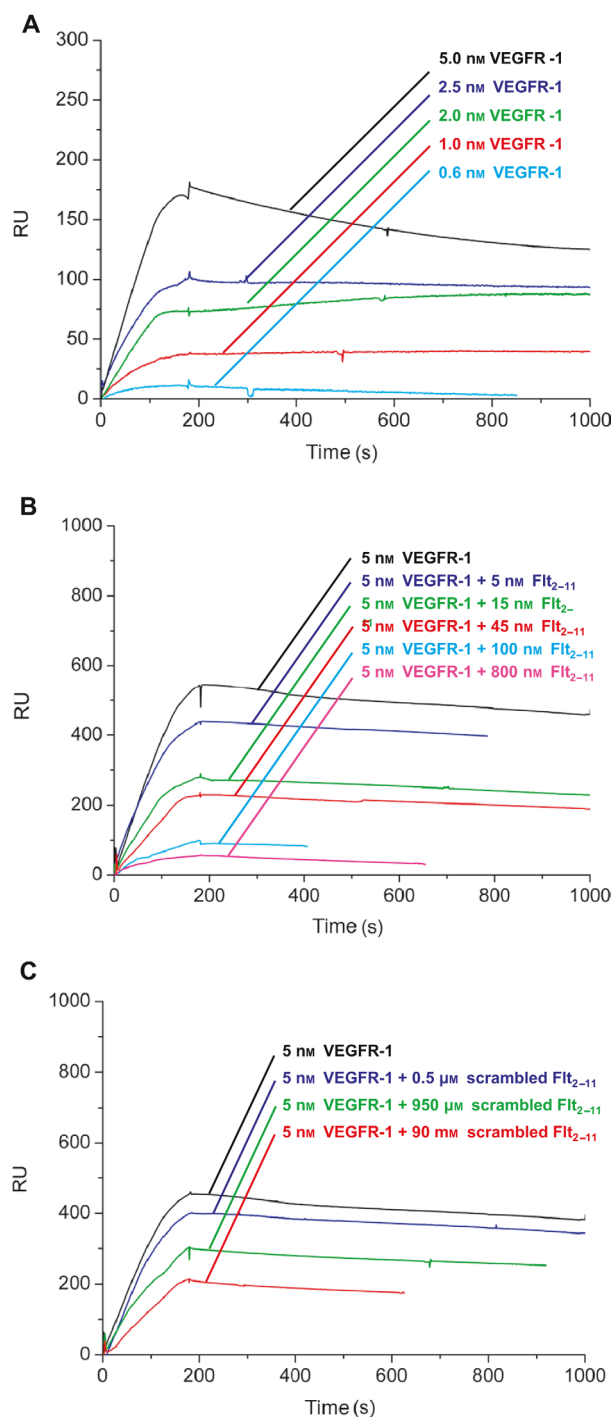


Fig. 1. Flt₂₋₁₁ peptide binds to NRP-1. (A) Solid-phase binding assay of biotinylated Flt₂₋₁₁ peptide on a plate coated with NRP-1, NRP-2, VEGFR-1 and BSA, as a negative control. (B) Solid-phase binding assay in the presence of different biotinylated peptides (P7, Flt₂₋₁₁, P4, P12 and B3) derived from the second Ig-like domain of VEGFR-1 [34,36], or in peptide absence (No add), on NRP-1-coated plates. Attached peptides were quantified by incubation with alkaline phosphatase-conjugated streptavidin and a colorimetric assay. Experiments were performed in triplicate and repeated at least three times, with comparable results. Representative experiments are shown. Data are reported as mean \pm SE of peptide adhesion with respect to control (peptide absence). Student's *t*-test: * $P \leq 0.05$; ** $P \leq 0.01$.

Since the Flt₂₋₁₁ peptide corresponds to a sequence within VEGFR-1 second Ig-like domain, we performed surface plasmon resonance (SPR) analyses to investigate whether Flt₂₋₁₁ peptide inhibited NRP-1 interaction with VEGFR-1. We found that Flt₂₋₁₁ peptide inhibited NRP-1 binding to VEGFR-1 with high efficiency ($K_i = 20$ nM; Fig. 2A,B). Inhibition of



NRP-1/VEGFR-1 interaction by Flt₂₋₁₁ peptide was also specific, given that a ‘scrambled’ Flt₂₋₁₁ peptide, containing the same residues as Flt₂₋₁₁ but in a different order, had no effect on NRP-1/VEGFR-1 interaction (Fig. 2C). Conversely, Flt₂₋₁₁ peptide did not detectably affect NRP-1 interaction with either $\alpha 5\beta 1$ integrin (Fig. 3A,B) or semaphorin 3A (Fig. 3C,D).

Fig. 2. Flt₂₋₁₁ peptide inhibits NRP-1 binding to VEGFR-1. SPR analysis of the interaction between VEGFR-1 and NRP-1 in peptide absence (A), or presence of Flt₂₋₁₁ peptide (B) or scrambled Flt₂₋₁₁ peptide (C). NRP-1 is immobilized on the sensor chip. (A) VEGFR-1 is injected at different concentrations (from bottom to top: 0.6 nM, cyan; 1 nM, red; 2 nM, green; 2.5 nM, blue; and 5 nM, black). Association and dissociation kinetic constants are $k_{on} = 1.2 \times 10^4 \text{ M}^{-1}\cdot\text{s}^{-1}$ and $k_{off} = 3 \times 10^{-4} \text{ s}^{-1}$; the thermodynamic dissociation constant is $K_D = 25 \pm 4 \text{ nM}$. (B) VEGFR-1 is injected at 5 nM together with peptide Flt₂₋₁₁ at different concentrations (from top to bottom: 0, black; 5 nM, blue; 15 nM, green; 45 nM, red; 100 nM, cyan; and 800 nM, magenta). Flt₂₋₁₁ peptide effectively inhibits NRP-1/VEGFR-1 interaction ($K_i = 20 \text{ nM}$). (C) VEGFR-1 is injected at 5 nM together with ‘scrambled’ Flt₂₋₁₁ peptide at different concentrations (from top to bottom: 0, black; 0.5 μM , blue; 950 μM , green; and 90 μM , red). Scrambled Flt₂₋₁₁ inhibits NRP-1/VEGFR-1 interaction only at high concentrations ($K_i = 10 \text{ nM}$).

NRP-1 is required for EC adhesion to sVEGFR-1

We had previously reported that Flt₂₋₁₁ peptide specifically interfered with EC adhesion to sVEGFR-1 but had no effect on EC adhesion to fibronectin, even if EC binding to both these extracellular matrix proteins is mediated by $\alpha 5\beta 1$ integrin [34]. We show here that this effect is specific, since the scrambled Flt₂₋₁₁ peptide does not affect EC adhesion on either sVEGFR-1 or fibronectin (Fig. 4A).

Taken together, the ability of Flt₂₋₁₁ peptide to (a) bind NRP-1 and inhibit NRP-1 interaction with VEGFR-1 reported above, and (b) specifically inhibit EC adhesion to sVEGFR-1, suggest that NRP-1 interaction with VEGFR-1 is required for ECs adhesion to sVEGFR-1 to occur.

To test this hypothesis, we silenced NRP-1 in ECs by small hairpin RNA (shRNA) interference.

We found, by real-time RT-PCR, that shRNA treatment reduced NRP-1 mRNA levels by about 60% (Fig. 4B). Additionally, FACS analysis showed that shRNA treatment strongly reduced NRP-1 protein expression, with respect to the levels observed in cells treated with control shRNA (Fig. 4C). Since NRP-1 was previously shown to be involved in the regulation of $\alpha 5\beta 1$ integrin trafficking [24], we evaluated integrin expression in our interfered cells. As shown in Fig. 4C, NRP-1 mRNA interference slightly reduced $\alpha 5\beta 1$ integrin membrane levels (by about 1/3).

Using NRP-1 interfered cells, we observed a reduction of EC adhesion both to fibronectin (47% reduction), in agreement with previously reported data [24], and to a greater extent, to sVEGFR-1 (65% reduction) (Fig. 5A). These results indicate that NRP-1 is required for effective EC binding to sVEGFR-1, and the reduction of EC adhesion to sVEGFR-1 is

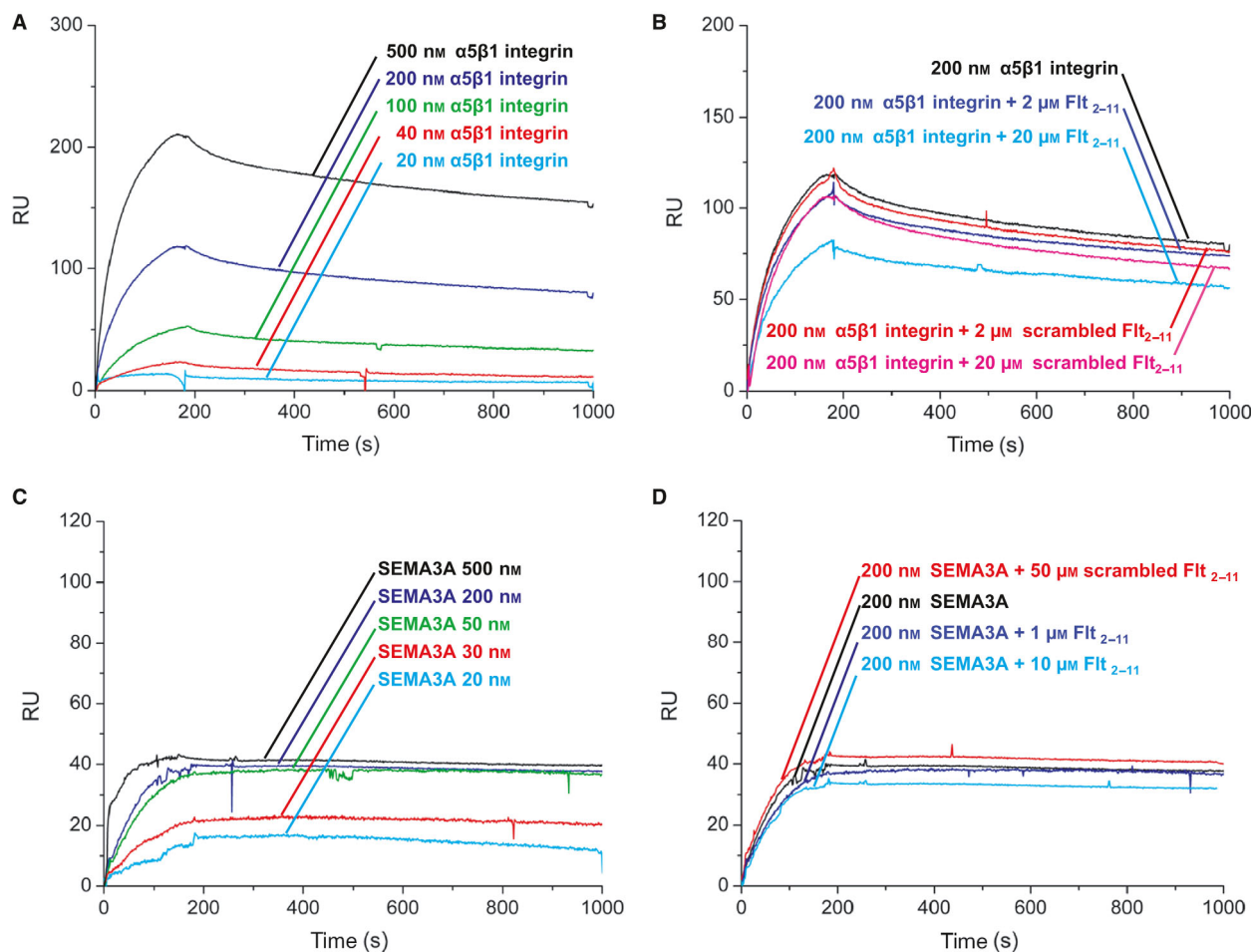


Fig. 3. Flt₂₋₁₁ peptide does not interfere with NRP-1 binding to either $\alpha 5\beta 1$ integrin or semaphorin 3A, in the absence or presence of Flt₂₋₁₁ peptide or 'scrambled' Flt₂₋₁₁. NRP-1 is immobilized on sensor chip. (A) $\alpha 5\beta 1$ integrin is injected at different concentrations (from bottom to top: 20 nM, cyan; 40 nM, red; 100 nM, green; 200 nM, blue; and 500 nM, black). Kinetic and thermodynamic parameters are: $k_{on} = 2.1 \times 10^4 \text{ M}^{-1} \cdot \text{s}^{-1}$; $k_{off} = 2.9 \times 10^{-4} \text{ s}^{-1}$; $K_D = 14 \pm 4 \text{ nM}$. (B) $\alpha 5\beta 1$ integrin is injected at 200 nM concentration together with either Flt₂₋₁₁ peptide or scrambled Flt₂₋₁₁ peptide at different concentrations (no peptides, black; Flt₂₋₁₁ peptide 2 M μ and 20 μ M, blue and cyan, respectively; scrambled Flt₂₋₁₁ peptide at 2 μ M and 20 μ M, red and purple, respectively). (C) Semaphorin 3A is injected at different concentrations (from bottom to top: 20 nM, cyan; 30 nM, red; 50 nM, green; 200 nM, blue; and 500 nM, black). Interaction parameters: $k_{on} = 3.7 \times 10^3 \text{ M}^{-1} \cdot \text{s}^{-1}$; $k_{off} = 9 \times 10^{-5} \text{ s}^{-1}$; $K_D = 24 \pm 6 \text{ nM}$. (D) Semaphorin 3A is injected at 200 nM, and peptide Flt₂₋₁₁ at different concentrations (no peptides, black; Flt₂₋₁₁ peptide 1 μ M and 10 μ M blue and cyan, respectively; scrambled Flt₂₋₁₁ peptide 50 μ M, red).

contributed by both an indirect role of NRP-1, which is exerted through modulation of $\alpha 5\beta 1$ integrin, and a direct role of NRP-1 in EC adhesion to sVEGFR-1. The reduction of EC adhesion to fibronectin, which is only determined by the indirect role of NRP-1, is less pronounced (Fig. 5A).

NRP-1 interaction with the soluble VEGFR-1 isoform is required for EC adhesion

To dissect whether interaction of NRP-1 with the transmembrane or the soluble isoform of VEGFR-1

was required for EC adhesion to sVEGFR-1, we performed EC adhesion assays by substituting sVEGFR-1 with a different adhesion substrate, named peptide 12. This is a seven amino acid-long peptide that, like Flt₂₋₁₁, maps on the second VEGFR-1 Ig-like domain and that we previously reported to be able to directly bind $\alpha 5\beta 1$ integrin and support EC adhesion, resulting into a pro-angiogenic stimulus [34].

In this assay, no sVEGFR-1 isoform is available, therefore tmVEGFR-1 is the only VEGFR-1 isoform that could interact with NRP-1. As shown in Fig. 5B, addition of Flt₂₋₁₁ peptide does not reduce EC adhesion

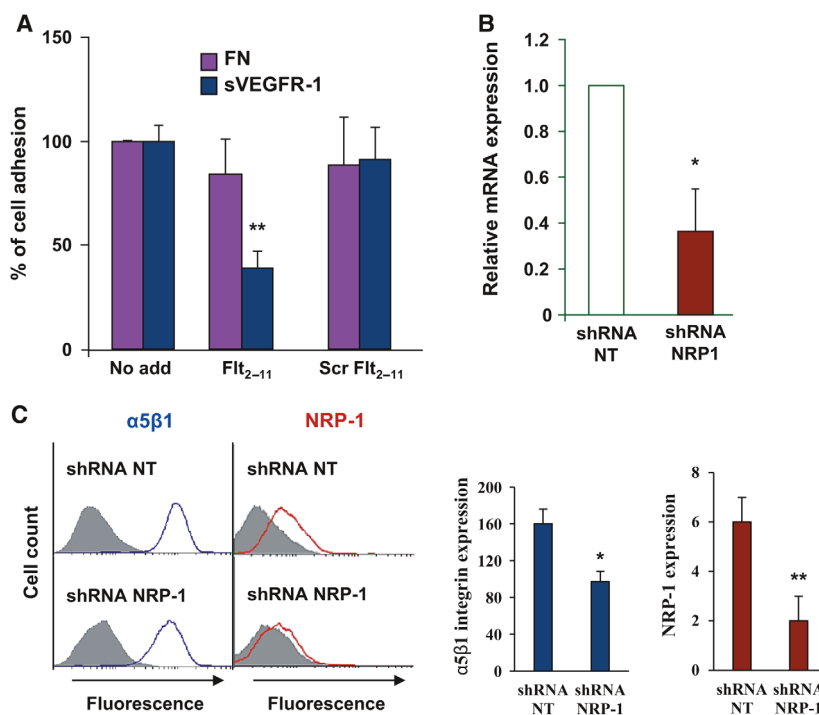


Fig. 4. Evaluation of RNA interference for NRP-1 in HUVECs. (A) EC adhesion to either sVEGFR-1 or fibronectin (FN) in the presence of Flt₂₋₁₁ peptide or scrambled (Scr) Flt₂₋₁₁ peptide or in the absence of any peptide (No add). Results are expressed as percentage of basal EC adhesion to each protein with respect to the control (No add). Student's *t*-test: ***P* < 0.01. (B) Real-time RT-PCR on total RNA extracted from ECs, either interfered for NRP-1 expression (shRNA NRP-1) or transfected with a shRNA for an unrelated, not-targeted gene (shRNA NT). Results are reported as relative fold expression with respect to shRNA NT-transfected cells and represent the mean ± SE of experiments performed in triplicate out of three independent determinations. (C) FACS analysis was performed to determine integrin α5β1 and NRP-1 levels in ECs interfered for NRP-1 expression (shRNA NRP-1) and transfected with a control shRNA (shRNA NT). Panels show the results of a representative experiment, and histograms indicate the quantification of α5β1 and NRP-1 expression, evaluated as variations in the geometric mean fluorescence intensity. Results represent the mean values ± SE of four independent determinations. In B and C, Student's *t*-test: **P* ≤ 0.05, ***P* ≤ 0.01.

to peptide 12, indicating that this process does not require a putative NRP-1 interaction with tmVEGFR-1. Additionally, EC adhesion to peptide 12 is not reduced by downregulation of NRP-1 expression by shRNA interference, indicating that this process does not require the presence of NRP-1 (Fig. 5B). Interestingly, cell adhesion to peptide 12 is increased in the presence of Flt₂₋₁₁ peptide (Fig. 5B).

To investigate the reasons underlying EC ability to adhere to peptide 12, but not to the whole sVEGFR-1, in the absence of NRP-1, we analysed the three-dimensional (3D) structure of the second VEGFR-1 Ig-like domain, which has been experimentally determined by X-ray crystallography in complex with VEGF-A165 [38]. This 3D structure comprises the whole peptide 12 sequence. Visual inspection and solvent accessible surface area measurement (see Table 1) indicated that peptide 12 residues Tyr220, Leu221, His223 and Arg224, which we previously

demonstrated to contribute the most to the interaction with α5β1 integrin [34], are buried within the second VEGFR-1 Ig-like domain. A conformational change of this domain, resulting in the exposure of these four residues, must therefore take place to allow α5β1 integrin interaction with, and EC adhesion to, sVEGFR-1.

EC adhesion assays to sVEGFR-1 or fibronectin in the presence of soluble NRP-1 were also performed to further define the role of this molecule. As shown in Fig. 5C, when soluble NRP-1 was added to the plates coated with either sVEGFR-1 or fibronectin prior to EC addition, EC adhesion to sVEGFR-1, but not to fibronectin, was impaired. These results indicate that soluble NRP-1, bound to coated sVEGFR-1, competes with the interaction between coated sVEGFR-1 and NRP-1 present on the EC membrane. On the other hand, when ECs were pretreated with soluble NRP-1, allowing it to bind to the tmVEGFR-1 isoform on

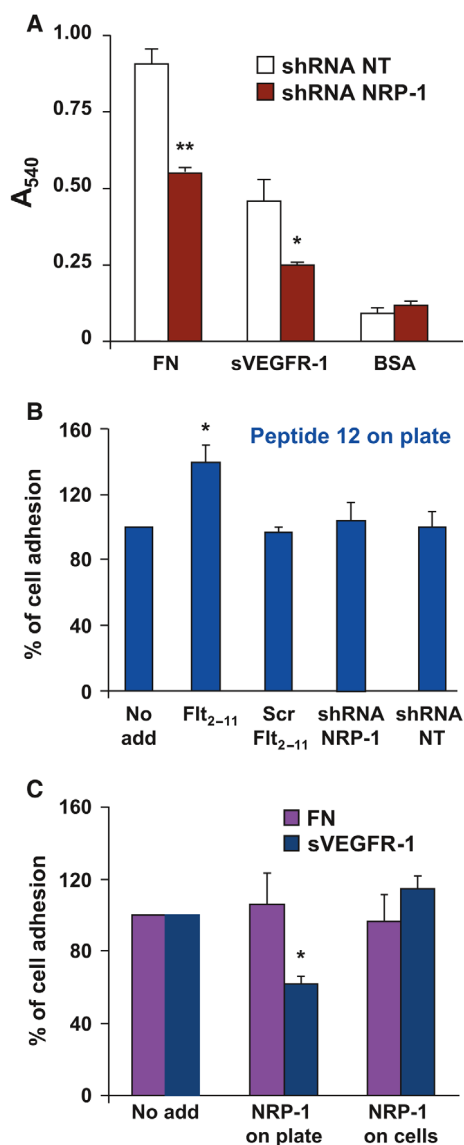


Fig. 5. NRP-1 interaction with sVEGFR-1 is required for EC adhesion to sVEGFR-1. (A) Adhesion of ECs, interfered for expression of NRP-1 (shRNA NRP-1), or of an unrelated, not-targeted gene (shRNA NT), to sVEGFR-1 or FN. Representative experiments performed in triplicate are shown; data are reported as mean \pm SE. Student's t-test: * $P \leq 0.05$; ** $P \leq 0.01$. Experiments were repeated at least three times with comparable results. (B) Adhesion of normal ECs or of ECs interfered with an unrelated, not-targeted gene (shRNA NT), to peptide 12, in the presence of Flt₂₋₁₁ peptide or Scr Flt₂₋₁₁ peptide, or in the absence of any peptide (No add). Results are expressed as percentage of basal EC adhesion to peptide 12. Student's t-test: * $P \leq 0.05$. (C) EC adhesion to sVEGFR-1 or FN, in the absence (No add) or in the presence of soluble NRP-1, incubated with either the substrate-coated plates (NRP-1 on plate), or with ECs prior to their addition in the adhesion assay (NRP-1 on cells). Results are expressed as percentage of basal EC adhesion on either sVEGFR-1 or FN, with respect to the controls (No add). Representative experiments performed in triplicate are shown; data are reported as mean \pm SE. Student's t-test: * $P \leq 0.05$. Experiments were repeated at least three times with comparable results.

second Ig-like domain of VEGFR-1 in complex with VEGF-A165, which has been experimentally determined by X-ray crystallography. Since we found that part of the region comprised within the Flt₂₋₁₁ peptide is involved in VEGF-A165 binding (Fig. 6A), we designed two additional peptides, eight and five-residue-long, respectively, by eliminating three or all the five Flt₂₋₁₁ peptide residues located in the VEGF-A165 binding region (Fig. 6A). Both Flt₂₋₁₁ derived peptides (*i.e.*, Flt₂₋₈ and Flt₂₋₅) were able to significantly inhibit EC adhesion to (Fig. 6B), and migration towards, sVEGFR-1 (Fig. 6C), to a similar extent as the Flt₂₋₁₁ peptide.

NRP-1 affinity for either sVEGFR-1 or $\alpha 5\beta 1$ integrin is higher than the affinity between sVEGFR-1 and $\alpha 5\beta 1$ integrin

The above-reported results demonstrate that NRP-1 binding to sVEGFR-1 is required for EC adhesion to sVEGFR-1, a process that we have previously demonstrated to be mediated by a direct interaction between sVEGFR-1 deposited in the extracellular matrix and $\alpha 5\beta 1$ integrin on EC membranes [31].

To investigate the interplay between these molecules, we compared the affinities measured for each pairwise interaction with one another. Interestingly, the interaction between sVEGFR-1 and $\alpha 5\beta 1$ integrin measured by SPR is one order of magnitude weaker ($K_D = 195 \pm 40$ nM; Fig. 7A) than NRP-1 interaction with either sVEGFR-1 ($K_D = 25 \pm 4$ nM; Fig. 2A) or

ECs, cell adhesion to either sVEGFR-1 or fibronectin was not detectably altered (Fig. 5C).

Taken together, these data indicate that the interaction between NRP-1 present on ECs, and sVEGFR-1 isoform in the extracellular matrix, supports sVEGFR-1 interaction with $\alpha 5\beta 1$ integrin and EC adhesion to sVEGFR-1. Conversely, NRP-1 interaction with tmVEGFR-1 does not appear to play a role in EC adhesion to sVEGFR-1.

A five-residue-long peptide is sufficient to impair EC adhesion and migration

To identify the shortest peptide sequence able to interfere with EC adhesion to and migration towards sVEGFR-1, we inspected the 3D structure of the

Table 1. Availability of peptide 12 residues for interaction. SASA (\AA^2) of peptide 12 residues in the isolated peptide 12 and in the context of the 3D structure of the second Ig-like domain of VEGFR-1 (PDB identifier: 1FLT, Resolution: 1.7 \AA). a.a.: amino acid type, three-letter code; Nb: residue number in the PDB file; chain x, chain y: name of the chains of the two sVEGFR-1 Ig-like domain 2 copies present in the experimental structure; Peptide, Domain and Diff: SASA of each residue and of the whole peptide 12 in the free state and in the context of the whole domain, and difference between these values, respectively. Residues previously shown to play an essential role in EC adhesion and/or $\alpha 5\beta 1$ integrin binding to sVEGFR-1 [34] are bold.

a.a.	Nb.	Chain X			Chain Y		
		Peptide	Domain	Diff	Peptide	Domain	Diff
ASN	219	185.72	25.56	160.16	187.86	31.39	156.47
TYR	220	216.75	4.15	212.6	221.19	5.36	215.83
LEU	221	175.74	64.17	111.57	169.71	66.21	103.5
THR	222	135.71	6.5	129.21	131.26	6.18	125.08
HIS	223	155.42	83.65	71.77	165.92	87.12	78.8
ARG	224	230.88	124.41	106.47	211.21	117.66	93.55
GLN	225	211.59	132.04	79.55	209.21	202.16	7.05
Peptide 12	219–225	1311.81	440.48	871.33	1296.36	516.08	780.28

$\alpha 5\beta 1$ integrin ($K_D = 14 \pm 4$ nM; Fig. 3A), whereas the strength of the latter interactions is comparable. These results indicate that, if a ternary complex was formed among these three molecules, NRP-1 interactions with sVEGFR-1 and $\alpha 5\beta 1$ integrin would have a stabilizing effect on sVEGFR-1 interaction with $\alpha 5\beta 1$ integrin.

To explore the possibility that a ternary complex among NRP-1, sVEGFR-1 and $\alpha 5\beta 1$ integrin is formed, we inspected the primary and tertiary structure of VEGFR-1 Ig-like domain II, whose 3D structure has been experimentally determined by X-ray crystallography in complex with VEGF-A165 (Fig. 7B). Residues belonging to Flt₂₋₁₁ peptide, which interacts with NRP-1, and peptide 12, which interacts with $\alpha 5\beta 1$ integrin, correspond to separate regions of both VEGFR-1 sequence (residues 164–174 and 219–225, respectively) and 3D structure (they partially overlap with β -strands C and H of Ig-like domain II, respectively) (Fig. 7B). In particular, the five-residue-long region of Flt₂₋₁₁ peptide, which is sufficient to inhibit EC adhesion and migration (Fig. 6A), maps on a sVEGFR-1 Ig-like domain II region opposite to that of peptide 12 (Fig. 7B). Thus, while neither $\alpha 5\beta 1$ integrin nor NRP-1 regions involved in the interaction with sVEGFR-1, or with each other, are known, formation of a complex among NRP-1, sVEGFR-1 and $\alpha 5\beta 1$ integrin cannot be excluded.

Figure 7C reports a schematic representation of the role of NRP-1 in EC adhesion to sVEGFR-1, and of the mechanism of action of the Flt₂₋₁₁ peptide, which have been proposed based on the results obtained in this work.

Discussion

In this study, we analyse the role played by NRP-1 in angiogenesis, by taking advantage of two previously

reported peptides, both of which map on the extracellular region of VEGFR-1 receptor.

First, we investigate in detail the mechanism underlying the anti-angiogenic activity of the Flt₂₋₁₁ peptide, the name of which indicates that it comprises eleven residues mapping on the second Ig-like domain of VEGFR-1 [35]. Flt₂₋₁₁ peptide had been originally reported to exert an anti-angiogenic activity, but the mechanism involved in this activity was not understood. However, Flt₂₋₁₁ peptide was demonstrated not to bind VEGF-A165 or interfere with VEGF-A165 binding to ECs [35]. Subsequently, we reported that Flt₂₋₁₁ peptide does not bind to $\alpha 5\beta 1$ integrin [34]. In the present work, we show that the Flt₂₋₁₁ peptide specifically binds to NRP-1 and disrupts NRP-1 interaction with sVEGFR-1. Additionally, we demonstrate that this peptide inhibits EC adhesion to, and migration towards, sVEGFR-1, two processes mediated by the interaction of sVEGFR-1 with $\alpha 5\beta 1$ integrin. These results indicate that NRP-1/sVEGFR-1 interaction is required for a productive sVEGFR-1/ $\alpha 5\beta 1$ integrin interaction to take place. Consequently, the previously reported anti-angiogenic effect of the Flt₂₋₁₁ peptide is likely to be mediated by the peptide ability to interfere with sVEGFR-1/NRP-1 binding, which results in the inhibition of the pro-angiogenic interaction between sVEGFR-1 and $\alpha 5\beta 1$ integrin.

The requirement of a sVEGFR-1/NRP-1 interaction for the efficient binding of sVEGFR-1 to $\alpha 5\beta 1$ integrin leads us to question the interplay among these three molecules during the EC adhesion process.

To answer this question, we take advantage of a different peptide previously studied by our group, named peptide 12, which also maps on the surface of VEGFR-1 second Ig-like domain, and mediates EC adhesion and $\alpha 5\beta 1$ integrin binding [34]. In the present

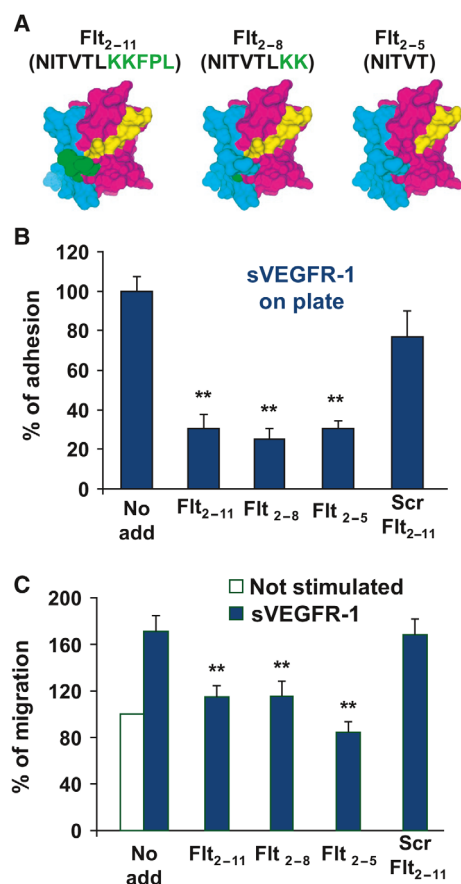


Fig. 6. Effect of Flt₂₋₈ and Flt₂₋₅ peptides on EC adhesion and migration. (A) SASA of the 3D structure of VEGFR-1 Ig-like domain II. Colour coding: green, residues comprised in the Flt₂₋₁₁ or Flt₂₋₈ peptide that are in contact with VEGF-A165; yellow, residues comprised in the Flt₂₋₁₁, Flt₂₋₈ or Flt₂₋₅ peptide that are not in contact with VEGF-A165; cyan and magenta, other VEGFR-1 residues that are and are not in contact with VEGF-A165, respectively. The images were generated using the INSIGHTII program (Accelrys Inc.). (B) EC adhesion to sVEGFR-1 in the presence of peptide Flt₂₋₁₁, Flt₂₋₈, Flt₂₋₅ or scrambled (Scr) Flt₂₋₁₁, or in the absence of any peptide (No add). Results are expressed as percentage of basal EC adhesion to sVEGFR-1. (C) Migration towards sVEGFR-1 in the presence of peptide Flt₂₋₁₁, Flt₂₋₈, Flt₂₋₅ or Scr Flt₂₋₁₁, or in the absence of any peptide (No add). Results are expressed as percentage of basal EC migration in the absence of any stimulus. In B and C, representative experiments performed in triplicate are shown; data are reported as mean \pm SE. Student's *t*-test: ***P* \leq 0.01, comparing peptide treated to untreated (No add) controls. Experiments were repeated at least three times with comparable results.

work, we show that ECs adhere to peptide 12 in the absence of NRP-1, and that this adhesion is not affected by the Flt₂₋₁₁ peptide. These results imply that α 5 β 1 integrin interaction with peptide 12 does not

require NRP-1 interaction with sVEGFR-1. EC ability to adhere to peptide 12, but not to the whole sVEGFR-1, in the absence of NRP-1, can be explained based on the analysis of the experimentally determined 3D structure of VEGFR-1 second Ig-like domain. In this structure, the four residues previously demonstrated to be essential for the interaction with α 5 β 1 integrin, namely Tyr220, Leu221, His223 and Arg224, are largely buried. To interact with α 5 β 1 integrin, VEGFR-1 needs to undergo a conformational change, leading to the exposure of these four residues. Therefore, the high-affinity sVEGFR-1/NRP-1 interaction may contribute to stabilize a sVEGFR-1 conformation where these residues are exposed, and available for the interaction with α 5 β 1 integrin, thus facilitating EC adhesion on sVEGFR-1. In agreement with this hypothesis, EC ability to adhere to peptide 12 in the absence of NRP-1 may be ascribed to the fact that in peptide 12 the four aforementioned residues are fully available for the interaction with α 5 β 1 integrin.

These observations also suggest that NRP-1/sVEGFR-1 interaction is not required to activate α 5 β 1 integrin-mediated signal transduction. As we have previously shown, EC adhesion to sVEGFR-1 does not activate canonical α 5 β 1 integrin signalling, such as phosphorylation of focal adhesion kinase or Shc, but acts through up-regulation of myristoylated alanine-rich C-kinase substrate and persistent activation of Rac1, due to the involvement of radixin and G α ₁₃ protein [32]. This special signalling pathway is also activated by EC adhesion to peptide 12 (data not shown), which is neither hampered by downregulation of NRP-1 expression through shRNA interference, nor by inhibition of NRP-1/sVEGFR-1 interaction by Flt₂₋₁₁ peptide.

Surprisingly, in the absence of sVEGFR-1 substrate, Flt₂₋₁₁ peptide increases cell adhesion to peptide 12. Based on the mechanism of action of Flt₂₋₁₁ peptide disclosed in this work, it is reasonable to speculate that Flt₂₋₁₁ peptide inhibits NRP-1 interaction with the transmembrane form of VEGFR-1, thus increasing the amount of NRP-1 available to exert the α 5 β 1 integrin cell adhesion-enhancing function, as previously observed [24].

To investigate the relative strength of interaction of NRP-1, sVEGFR-1 and α 5 β 1 integrin with one another, we perform *in vitro* SPR experiments. The results of these experiments indicate that the *K*_D of both interactions involving NRP-1, namely NRP-1/sVEGFR-1 and NRP-1/ α 5 β 1 integrin, are 10-fold lower than that of the sVEGFR-1/ α 5 β 1 integrin interaction. In case a ternary complex was formed among these molecules, NRP-1 would have a stabilizing role

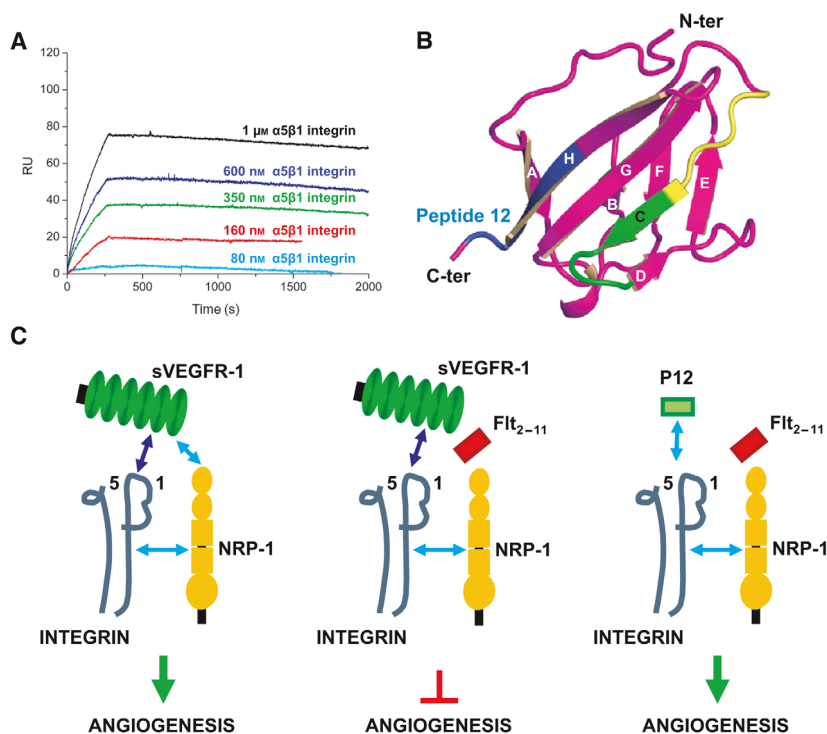


Fig. 7. sVEGFR-1/ $\alpha 5\beta 1$ integrin interaction. (A) SPR analysis of the interaction between sVEGFR-1 and $\alpha 5\beta 1$ integrin. sVEGFR-1 is immobilized on sensor chips and $\alpha 5\beta 1$ integrin is injected at different concentrations (from bottom to top: 80 nM, cyan; 160 nM, red; 350 nM, green; 600 nM, blue; and 1 μ M, black). Interaction parameters: $k_{on} = 1.5 \times 10^3 \text{ M}^{-1} \cdot \text{s}^{-1}$; $k_{off} = 2.9 \times 10^{-4} \text{ s}^{-1}$; $K_D = 195 \pm 40 \text{ nM}$. (B) Secondary structure representation of the 3D structure of VEGFR-1 Ig-like domain II. β -strands are represented by arrows and labelled from A to H; loops are shown as tubular ribbons; the N- and C-terminal ends of the domain are indicated by labels. Colour coding: peptide 12 (interacting with $\alpha 5\beta 1$ integrin) is blue; Flt₂₋₁₁ peptide (interacting with NRP-1) is yellow in the five-residue NITVT region corresponding to the Flt₂₋₅ peptide (see text), and green in the remaining six-residues region; the rest of the domain is magenta. (C) Proposed mechanism of action of Flt₂₋₁₁ peptide. Left: Light blue arrows indicate the high-affinity interactions: (i) between NRP-1 (yellow) and $\alpha 5\beta 1$ integrin (black) on the EC membrane; and (ii) between NRP-1 on the EC membrane and the sVEGFR-1 substrate (green). The dark blue arrow indicates the low-affinity interaction between $\alpha 5\beta 1$ integrin on the EC membrane and the sVEGFR-1 substrate. The low-affinity interaction is stabilized by the two high-affinity interactions, and the angiogenic stimulus is triggered. Centre: The Flt₂₋₁₁ peptide inhibits the high-affinity interaction between NRP-1 on the EC membrane and the sVEGFR-1 substrate. The low-affinity interaction between $\alpha 5\beta 1$ integrin on ECs and the sVEGFR-1 substrate is not sufficiently stable to trigger the angiogenic stimulus that starts upon integrin engagement. Right: The affinity of the interaction between $\alpha 5\beta 1$ integrin (black) on the EC membrane and the P12 peptide substrate (light blue arrow) is high enough that additional stabilizing interactions are not required. Consequently, the $\alpha 5\beta 1$ integrin/P12 peptide interaction takes place both in the presence and in the absence of the Flt₂₋₁₁ peptide.

on the sVEGFR-1/ $\alpha 5\beta 1$ integrin interaction. Analysis of sVEGFR-1 Ig-like domain 2 sequence and structure indicates that Flt₂₋₁₁ peptide and peptide 12 residues, which bind NRP-1 and $\alpha 5\beta 1$ integrin, respectively, are not overlapping. Therefore, a simultaneous interaction involving all three molecules is possible. Indeed, NRP-1 has been reported to be involved in ternary complexes with other macromolecules. As an example, NRP-1 and plexin 1 form a complex whose affinity for semaphorin 3A is enhanced with respect to each component [41]. Additionally, NRP-1 binds PDGF-D and acts as a co-receptor, enhancing the formation of a complex between the growth factor and PDGFR β [42].

Further, $\beta 3$ integrin negatively regulates VEGF-A165-mediated angiogenesis by limiting the interaction of NRP-1 with VEGFR-2 [43]. Unfortunately, our attempts at isolating a ternary complex formed by NRP-1, sVEGFR-1 and $\alpha 5\beta 1$ integrin in ECs have not been successful so far.

Because of its peculiar mechanism of action, the Flt₂₋₁₁ peptide is an attractive lead for the development of anti-angiogenic compounds for therapeutic applications. Indeed, most of the previously developed therapeutics for pathological angiogenesis target VEGF-A165 interaction with transmembrane receptors and determine a reduction of VEGFR-2-mediated

signalling [44,45]. Small peptides that inhibit VEGF-A165 binding to NRP-1 hamper tumour growth and angiogenesis in breast cancer [46] and lung carcinoma [47] animal models. Anti-NRP-1 antibodies enhance the antitumor effects of anti-VEGF-A165 antibodies in a mouse xenograft model [48]. Inhibition of NRP-1 interaction with placenta growth factor has antitumor effects in a mouse model of medulloblastoma [46]. In the developing retina, the combination of anti-NRP-1 and anti-VEGF-A165 antibodies results in enhanced blood vessel regression [48]. A peptide interfering with VEGF-A165 binding to NRP-1 suppresses angiogenesis in experimental arthritis [49]. Conversely, the anti-angiogenic effect of the Flt₂₋₁₁ peptide is not mediated by inhibition of NRP-1 binding to VEGF family members, and subsequent reduction of signalling mediated by transmembrane VEGFRs [35], but by a novel mechanism, consisting in the inhibition of NRP-1/sVEGFR-1 interaction. Therefore, compounds acting with the same mechanism as Flt₂₋₁₁ peptide could be used as an alternative to classic anti-angiogenic molecules or in synergy with them in combined, more effective protocols.

As a first step to develop such anti-angiogenic agents, in this work we design shorter variants of Flt₂₋₁₁ peptide and test their biological activity. Analysis of the 3D structure of VEGFR-1 second Ig-like domain in complex with VEGF-A165, which has been experimentally determined by X-ray crystallography, revealed that some of the residues present in the Flt₂₋₁₁ peptide are involved in VEGF-A165 binding. To further reduce any chance of interference with VEGF-A165 activity, we designed two Flt₂₋₁₁ peptide variants comprising the first eight, and the first five, N-terminal residues, and named them Flt₂₋₈ and Flt₂₋₅, respectively. Both peptides result to be able to impair $\alpha 5\beta 1$ integrin-mediated EC adhesion to, and migration towards, sVEGFR-1 with an efficacy comparable to that of the parent eleven-residue Flt₂₋₁₁ peptide. Consequently, both peptides, and especially the five-residue Flt₂₋₅ peptide, represent novel potential angiogenesis inhibitors or lead compounds, based on which non-peptide molecules acting with the same mechanism may be developed.

In this work, we also find that Flt₂₋₁₁ peptide directly interacts with NRP-2. This protein has been previously shown to take part in a ternary complex with VEGFR-1 and VEGF-A165 [27]. However, NRP-2 and VEGFR-1 were not demonstrated to directly interact with each other. Interestingly, NRP-2 has been shown to interact with $\alpha 5\beta 1$ integrin and have a role in modulating cell/cell and cell/matrix adhesion [39,40]. Further studies will be required to elucidate the biological role of the NRP-2/VEGFR-1

interaction, and whether the two molecules interact directly or through VEGF-A165.

In summary, the results presented in this work demonstrate that the previously reported, direct NRP-1/sVEGFR-1 interaction is required for both EC adhesion to sVEGFR-1 and EC migration towards sVEGFR-1. Moreover, we discovered that the previously reported anti-angiogenic Flt₂₋₁₁ peptide inhibits the NRP-1/sVEGFR-1 interaction. This led to the development of two shorter peptides, named Flt₂₋₈ and Flt₂₋₅, both of which hamper EC adhesion to, and migration towards, sVEGFR-1 by inhibiting NRP-1/sVEGFR-1 interaction as well. This mechanism of action does not involve the inhibition of VEGF-A165 binding to its transmembrane receptors. Therefore, the peptides studied in this work are expected to act synergistically with classic anti-angiogenic agents and may be used in combination therapies for the treatment of tumours and other processes associated with pathological angiogenesis.

Materials and methods

Reagents

Recombinant human VEGFR-1/Fc (321-FL-050), human NRP-1 (3870-N1) and human NRP-2/Fc (2215-N2) were purchased from R&D Systems (Minneapolis, MN, USA). Fibronectin (F1141) and gelatin (G1393) were obtained from Sigma-Aldrich (St Louis, MO, USA). Purified $\alpha 5\beta 1$ integrin (CC1052), octyl- β -D-glucopyranoside formulation, was from Merck Millipore (Billerica, MA, USA). Peptide synthesis was carried out by Primm (Milan, Italy). Flt₂₋₁₁ peptide sequence was NITVTLKKFPL and scrambled Flt₂₋₁₁ peptide sequence was LVPLKIKNTFT.

Cell culture

Human umbilical vein endothelial cells (HUVEC) were isolated from freshly delivered umbilical cords, as previously described [50], cultured in Endothelial Cell Growth Medium-2 Kit from Clonetics (EGM-2, CC4176, Lonza, Basel, Switzerland), and used up to passage 6. For functional assays, HUVEC were resuspended in Endothelial Basal Medium-2 (EBM-2, CC3156, Lonza). A pool of cells derived from four different individuals was used.

Solid-phase binding assays

Immunological 96-multiwell plates were coated overnight at 4 °C with saturating amounts ($2 \mu\text{g}\cdot\text{mL}^{-1}$) of human NRP-1, human NRP-2/Fc, or human sVEGFR-1/Fc, in 25 mM Tris/HCl, 150 mM NaCl, 1 mM MgCl_2 (buffer A). Plates

were then blocked for 2 h at room temperature with 1% BSA/PBS. Biotinylated Flt₂₋₁₁ peptide or other biotinylated sVEGFR-1-derived peptides [34] were then added to a final concentration of 500 µg·mL⁻¹ for 1 h at room temperature. After three washes with buffer A, streptavidin-alkaline phosphatase-conjugated and the appropriate substrate (4-nitrophenylphosphate, Roche Diagnostics, Basel, Switzerland) were then used for detection of bound peptides. Absorbance was determined at 405 nm, using a Microplate reader 3550-UV (Bio-Rad, Hercules, CA, USA). Experiments were performed in triplicate and repeated at least three times with comparable results.

Cell adhesion assay

Solid support for adhesion assay was prepared by incubating immunological 96-multiwell plates with 20 µg·mL⁻¹ VEGFR-1/Fc chimera, or fibronectin solubilized in PBS. After 2 h, the coating solution was removed, and the well surface was blocked with 3% BSA in PBS for 18 h, before plating ECs in serum-free medium at 3 × 10⁴ cells per well. After incubation at 37 °C for 1 h, the wells were washed with PBS and attached cells were fixed with 3% formaldehyde and stained with 0.5% crystal violet. Attachment efficiency was determined by quantitative dye extraction and spectrophotometric measurement of the absorbance at 540 nm, using a Microplate reader 3550-UV (Bio-Rad). In competition experiments, peptides Flt₂₋₁₁, scrambled Flt₂₋₁₁, Flt₂₋₈ or Flt₂₋₅, at 20 µg·mL⁻¹, were added during the adhesion assay. Adhesion to peptide 12 was carried out by using maleic anhydride activated microplates (Reacti-Bind, Pierce, Rockford, IL, USA) coated with 500 µg·mL⁻¹ of the peptide. Experiments were performed in triplicate and repeated at least three times with comparable results.

RNA interference

MISSION Lentiviral Transduction Particle system was used (Sigma-Aldrich). Subconfluent HUVEC were infected at a multiplicity of infection (MOI) = 1, with either NRP-1 shRNA (SHCLNV-NM 003873, clone TRCN000030 0917, Sigma-Aldrich) or an unrelated, not-targeted non-mammalian shRNA (Sigma-Aldrich). After 24 h from infection, cell medium was changed with medium supplemented with 0.6 µM puromycin, to select cells infected with the virus containing the shRNA sequences.

After one week, interfered cells were used in cell adhesion assays, as described above. To evaluate levels of NRP-1 mRNA expression in silenced cells, real-time RT-PCR was performed. Total RNA was extracted from interfered cells, and cDNA was obtained using Superscript III First-Strand System (Invitrogen, Carlsbad, CA, USA), according to the manufacturer's protocol. Real-time RT-PCR was performed by the dual-labelled fluorogenic probe method,

using ABI Prism 7000 sequence detector (Perkin Elmer, Groningen, The Netherlands). Expression levels were calculated by the relative standard curve methods. Primers used were: NRP-1 forward 5'-GCCACAGTGGAAACAGGTGAT-3' and reverse 5'-GGAAACTCTGATTGTATGGTGCTG-3'; β-actin forward 5'-CATCGAGCACGGCATCGTCA-3' and reverse 5'-TAGCACAGCCTGGATGCAAC-3'.

Flow cytometry analysis

Cells were harvested, allowed to recover for two hours in a rotating wheel at room temperature and washed with PBS. Aliquots of 5 × 10⁵ cells were then incubated on ice in 2% BSA/PBS for 30 min with the following mouse monoclonal antibodies. For integrin α5β1 labelling, we used 1 µg of anti-α5β1 (MAB1969, Chemicon International, Temecula, CA, USA), washed with PBS and incubated with a secondary goat anti-mouse IgG (Fc specific)-FITC antibody (1 : 100, F2772, Sigma-Aldrich) on ice in 2% BSA/PBS for 30 min. For NRP-1 labelling, we used 10 µL of anti-human NRP-1-PE (CD304-PE, Miltenyi Biotec, Bergisch Gladbach, Germany) or mouse IgG1 control-PE (Becton Dickinson, Franklin Lakes, NJ, USA). After washing with PBS, cells were analysed using a FACScan flow cytometer (Becton & Dickinson).

Migration assays

Cell migration was analysed using Boyden chambers equipped with 8 µm pore diameter polycarbonate filters (Nuclepore, Whatman Incorporated, Clifton, NJ, USA). Human sVEGFR-1 stimulus (5 µg·mL⁻¹) for chemotaxis was added to the lower chamber and HUVEC (1.5 × 10⁵) were loaded into the upper chamber. To test the effect of peptides Flt₂₋₁₁, scrambled Flt₂₋₁₁, Flt₂₋₈ or Flt₂₋₅ on cell migration, cells were preincubated for 30 min at room temperature in migration medium (0.1% BSA in EBM-2/heparin medium) alone (No add) or containing one of the peptides at 40 µM concentration. Cells were then loaded into the Boyden chambers without removing the peptides, and migration towards sVEGFR-1 was analysed. After 2-h incubation in a CO₂ incubator at 37 °C, filters were removed, cells were fixed in 3% paraformaldehyde in PBS and stained in 0.5% crystal violet. Cells from the upper surface were removed by wiping with a cotton swab, and the chemotactic response was determined by counting the migrating cells attached to the lower surface of the filter in 12 randomly selected microscopic fields (×200 magnification) per experimental condition. Quantification was performed by two independent observers, blinded to the examined condition. Experiments were performed in triplicate and repeated at least three times with comparable results.

SPR measurements

SPR experiments were carried out using a BIACORE X system (Biacore AB, Uppsala, Sweden). The sensor chips (CM5, Biacore AB) were chemically activated by injection of 35 μL of a 1 : 1 mixture of *N*-hydroxysuccinimide (50 mM) and *N*-ethyl-*N'*-(3-dimethylaminopropyl)carbodiimide (200 mM) at a flow rate of 5 $\mu\text{L}\cdot\text{min}^{-1}$ [51]. For experiments where VEGFR-1/Fc is the immobilized ligand, the procedure described in [52] was followed. Briefly, protein A was immobilized using amine coupling with *N*-ethyl-*N'*-(3-dimethylaminopropyl)carbodiimide hydrochloride and *N*-hydroxysuccinimide to a density of 1000–2000 resonance units (RU). The remaining *N*-hydroxysuccinimide ester groups were blocked by injecting 1 M ethanolamine hydrochloride (35 μL). Recombinant human VEGFR-1/Fc was captured to approximately 200 RU. Interaction with analytes was achieved in HEPES-buffered saline (10 mM HEPES, pH 7.4; 150 mM NaCl; 0.005% surfactant P20). For association measurements, the analyte was injected at a rate of 20 $\text{mL}\cdot\text{min}^{-1}$. Dissociation was obtained with HEPES-buffered saline applied over the surface at 20 $\text{mL}\cdot\text{min}^{-1}$ for 30 min. Recombinant human NRP-1 was immobilized on the activated sensor chip via amine coupling. The reaction was carried out in 20 mM sodium acetate at pH 5.0, which is about 2 points below the theoretical NRP-1 isoelectric point calculated using the program pI-tool [53]. The remaining *N*-hydroxysuccinimide ester groups were blocked by injecting 1 M ethanolamine hydrochloride (35 μL). Interaction with the analyte was achieved in HEPES-buffered saline. For association measurements, the soluble ligand was injected at a rate of 30 $\text{mL}\cdot\text{min}^{-1}$. Dissociation was obtained with HEPES-buffered saline applied over the surface at 30 $\text{mL}\cdot\text{min}^{-1}$ for 30 min. In control experiments, the sensor chip was treated as described above in the absence of immobilized proteins.

RU express the mass concentration-dependent changes in the observed SPR signal, that is, the refractive index on the sensor chip surface. Changes in this signal are determined by the interaction between the immobilized protein (i.e., either NRP-1 or VEGFR-1) with the analyte protein (i.e., VEGFR-1/Fc, $\alpha 5\beta 1$ integrin or semaphorin 3A). Typically, a response change of 1000 RU corresponds to a change in the surface concentration on the sensor chip of about 1 ng of protein per mm^2 . Global fitting analyses of association and dissociation data for all ligand concentrations were carried out using BIAEVALUATION software 3.0 (Biacore, Uppsala, Sweden), which allows the ratio between association and dissociation constants ($k_{\text{on}}/k_{\text{off}}$) to be accurately determined. A simple 1 : 1 Langmuir model was employed to fit the data, where: $A + B \leftrightarrow AB$; A: analyte; B: ligand; AB: complex between A and B; k_{on} : association rate constant ($\text{M}^{-1}\cdot\text{s}^{-1}$); k_{off} : dissociation rate constant (s^{-1}). Scatchard analysis of R_{eq} dependence on analyte concentration was also performed to calculate the equilibrium dissociation constant.

Sequence and structure analysis

The 3D structure of the second VEGFR-1 Ig-like domain in complex with VEGF [38] was downloaded from the Protein Data Bank (PDB: www.rcsb.org) [54] and analysed using INSIGHTII (Accelrys Inc.) and Swiss-PDBViewer [55] (<http://www.expasy.org/spdbv/>). Solvent accessible surface area (SASA) was calculated using Naccess (<http://wolf.bms.umist.ac.uk/naccess/>).

Statistical analysis

Statistical significance of the differences between pairs of groups was assessed by two-tailed Student's *t*-test. Differences were statistically significant when $P < 0.05$.

Acknowledgements

Funding was provided by the Italian Ministry of Health (projects RC3.3-2018-2638151 and RC3.5-2019-2755065) and by the Italian Ministry of Education, University and Research (MIUR) as a Scientific Research Program of Relevant National Interest (PRIN 2017) entitled 'Protein Bioinformatics for Human Health' (grant no. 2017483NH8_005). Open Access Funding provided by Consiglio Nazionale delle Ricerche within the CRUI-CARE Agreement. [Correction added on 3 June 2022, after first online publication: CRUI funding statement has been added.]

Conflict of interest

The authors declare that they have no conflicts of interest with the contents of this article. The sources of financial support for the conduct of the research and preparation of the article did not perform any role in study design; in the collection, analysis and interpretation of data; in the writing of the report and in the decision to submit the article for publication.

Author contributions

GC designed SPR experiments, performed part of them, analysed results and wrote the paper. CMF designed cell adhesion experiments, performed part of them, analysed results and wrote the paper. PML designed cell migration experiments, analysed results and revised the paper. MU performed part of the SPR experiments. FR performed cell migration experiments. PDM performed part of the Bioinformatics analyses. AO performed part of the cell adhesion experiments. VM designed Bioinformatics analyses, performed part of them, analysed results and wrote the paper.

Peer Review

The peer review history for this article is available at <https://publons.com/publon/10.1111/febs.16119>.

References

- Shimizu M, Murakami Y, Suto F & Fujisawa H (2000) Determination of cell adhesion sites of neuropilin-1. *J Cell Biol* **148**, 1283–1293.
- He Z & Tessier-Lavigne M (1997) Neuropilin is a receptor for the axonal chemorepellent Semaphorin III. *Cell* **90**, 739–751.
- Kolodkin AL, Levenson DV, Rowe EG, Tai YT, Giger RJ & Ginty DD (1997) Neuropilin is a semaphorin III receptor. *Cell* **90**, 753–762.
- Migdal M, Huppertz B, Tessler S, Comforti A, Shibuya M, Reich R, Baumann H & Neufeld G (1998) Neuropilin-1 is a placenta growth factor-2 receptor. *J Biol Chem* **273**, 22272–22278.
- Soker S, Takashima S, Miao HQ, Neufeld G & Klagsbrun M (1998) Neuropilin-1 is expressed by endothelial and tumor cells as an isoform-specific receptor for vascular endothelial growth factor. *Cell* **92**, 735–745.
- Takagi S, Kasuya Y, Shimizu M, Matsuura T, Tsuboi M, Kawakami A & Fujisawa H (1995) Expression of a cell adhesion molecule, neuropilin, in the developing chick nervous system. *Dev Biol* **170**, 207–220.
- Chu W, Song X, Yang X, Ma L, Zhu J, He M, Wang Z & Wu Y (2014) Neuropilin-1 promotes epithelial-to-mesenchymal transition by stimulating nuclear factor-kappa B and is associated with poor prognosis in human oral squamous cell carcinoma. *PLoS One* **9**, e101931.
- Luo M, Hou L, Li J, Shao S, Huang S, Meng D, Liu L, Feng L, Xia P, Qin T *et al.* (2016) VEGF/NRP-1 axis promotes progression of breast cancer via enhancement of epithelial-mesenchymal transition and activation of NF-kappa B and beta-catenin. *Cancer Lett* **373**, 1–11.
- Yaqoob U, Cao S, Shergill U, Jagavelu K, Geng Z, Yin M, de Assuncao TM, Cao Y, Szabolcs A, Thorgeirsson S *et al.* (2012) Neuropilin-1 stimulates tumor growth by increasing fibronectin fibril assembly in the tumor microenvironment. *Cancer Res* **72**, 4047–4059.
- Xu J & Xia J (2013) NRP-1 silencing suppresses hepatocellular carcinoma cell growth in vitro and in vivo. *Exp Ther Med* **5**, 150–154.
- Chaudhary B, Khaled Y, Ammori B & Elkord E (2014) Neuropilin-1: function and therapeutic potential in cancer. *Cancer Immunol Immunother* **63**, 81–99.
- Cantuti-Castelvetri L, Ojha R, Pedro LD, Djannatian M, Franz J, Kuivanen S, van der Meer F, Kallio K, Kaya T, Anastasina M *et al.* (2020) Neuropilin-1 facilitates SARS-CoV-2 cell entry and infectivity. *Science* **370**, 856–860.
- Daly JL, Simonetti B, Klein K, Chen KE, Williamson MK, Anton-Plagaro C, Shoemark DK, Simon-Gracia L, Bauer M, Hollandi R *et al.* (2020) Neuropilin-1 is a host factor for SARS-CoV-2 infection. *Science* **370**, 861–865.
- Gu C, Limberg BJ, Whitaker GB, Perman B, Leahy DJ, Rosenbaum JS, Ginty DD & Kolodkin AL (2002) Characterization of neuropilin-1 structural features that confer binding to semaphorin 3A and vascular endothelial growth factor 165. *J Biol Chem* **277**, 18069–18076.
- Yelland T & Djordjevic S (2016) Crystal structure of the neuropilin-1 MAM domain: completing the neuropilin-1 ectodomain picture. *Structure* **24**, 2008–2015.
- Cai H & Reed RR (1999) Cloning and characterization of neuropilin-1-interacting protein: a PSD-95/Dlg/ZO-1 domain-containing protein that interacts with the cytoplasmic domain of neuropilin-1. *J Neurosci* **19**, 6519–6527.
- Grun D, Adhikary G & Eckert R (2016) VEGF-A acts via neuropilin-1 to enhance epidermal cancer stem cell survival and formation of aggressive and highly vascularized tumors. *Oncogene* **35**, 4379–4387.
- Pagani E, Ruffini F, Antonini Cappellini G, Scoppola A, Fortes C, MARCHETTI P, Graziani G, D'Atri S & Lacal PM (2016) Placenta growth factor and neuropilin-1 collaborate in promoting melanoma aggressiveness. *Int J Oncol* **48**, 1581–1589.
- Peach CJ, Mignone VW, Arruda MA, Alcobia DC, Hill SJ, Kilpatrick LE & Woolard J (2018) Molecular pharmacology of VEGF-A isoforms: binding and signalling at VEGFR2. *Int J Mol Sci* **19**, 1264.
- Gluzman-Poltorak Z, Cohen T, Herzog Y & Neufeld G (2000) Neuropilin 2 and neuropilin-1 are receptors for VEGF165 and PlGF-2, but only neuropilin-2 functions as a receptor for VEGF145. *J Biol Chem* **275**, 18040–18045.
- Murga M, Fernandez-Capetillo O & Tosato G (2005) Neuropilin-1 regulates attachment in human endothelial cells independently of vascular endothelial growth factor receptor-2. *Blood* **105**, 1992–1999.
- Kawasaki T, Kitsukawa T, Bekku Y, Matsuda Y, Sanbo M, Yagi T & Fujisawa H (1999) A requirement for neuropilin-1 in embryonic vessel formation. *Development* **126**, 4895–4902.
- Kitsukawa T, Shimono A, Kawakami A, Kondoh H & Fujisawa H (1995) Overexpression of a membrane protein, neuropilin, in chimeric mice causes anomalies in the cardiovascular system, nervous system and limbs. *Development* **121**, 4309–4318.
- Valdembri D, Caswell PT, Anderson KI, Schwarz JP, Konig I, Astanina E, Caccavari F, Norman JC,

- Humphries MJ, Bussolino F *et al.* (2009) Neuropilin-1/GIPC1 signaling regulates $\alpha 5\beta 1$ integrin traffic and function in endothelial cells. *PLoS Biol* **7**, 115–132.
- 25 Fukasawa M, Matsushita A & Korc M (2007) Neuropilin-1 interacts with integrin $\beta 1$ and modulates pancreatic cancer cell growth, survival and invasion. *Cancer Biol Ther* **6**, 1173–1180.
- 26 Fuh G, Garcia KC & de Vos AM (2000) The interaction of neuropilin-1 with vascular endothelial growth factor and its receptor Flt-1. *J Biol Chem* **275**, 26690–26695.
- 27 Neufeld G, Kessler O & Herzog Y (2002) The interaction of neuropilin-1 and neuropilin-2 with tyrosine kinase receptors for VEGF. *Adv Exp Med Biol* **515**, 81–90.
- 28 Inoue T, Kibata K, Suzuki M, Nakamura S, Motoda R & Orita K (2000) Identification of a vascular endothelial growth factor (VEGF) antagonist, sFlt-1, from a human hematopoietic cell line NALM-16. *FEBS Lett* **469**, 14–18.
- 29 Kendall RL, Wang G & Thomas KA (1996) Identification of a natural soluble form of the vascular endothelial growth factor receptor, FLT-1, and its heterodimerization with KDR. *Biochem Biophys Res Commun* **226**, 324–328.
- 30 Sela S, Itin A, Natanson-Yaron S, Greenfield C, Goldman-Wohl D, Yagel S & Keshet E (2008) A novel human-specific soluble vascular endothelial growth factor receptor 1: cell type-specific splicing and implications to vascular endothelial growth factor homeostasis and preeclampsia. *Circ Res* **102**, 1566–1574.
- 31 Orecchia A, Lacal PM, Schietroma C, Morea V, Zambruno G & Failla CM (2003) Vascular endothelial growth factor receptor-1 is deposited in the extracellular matrix by endothelial cells and is a ligand for the $\alpha 5\beta 1$ integrin. *J Cell Sci* **116**, 3479–3489.
- 32 Orecchia A, Mettouchi A, Uva P, Simon GC, Arcelli D, Avitabile S, Ragone G, Meneguzzi G, Pfenninger KH, Zambruno G *et al.* (2014) Endothelial cell adhesion to soluble vascular endothelial growth factor receptor-1 triggers a cell dynamic and angiogenic phenotype. *FASEB J* **28**, 692–704.
- 33 Faycal CA, Brambilla E, Agorreta J, Lepeltier N, Jacquet T, Lemaitre N, Emadali A, Lucas A, Lacal PM, Montuenga L *et al.* (2018) The sVEGFR1-i13 splice variant regulates $\alpha \beta 1$ integrin/VEGFR autocrine loop involved in the progression and the response to anti-angiogenic therapies of squamous cell lung carcinoma. *Br J Cancer* **118**, 1596–1608.
- 34 Soro S, Orecchia A, Morbidelli L, Lacal PM, Morea V, Ballmer-Hofer K, Ruffini F, Ziche M, D'Atri S, Zambruno G *et al.* (2008) A proangiogenic peptide derived from vascular endothelial growth factor receptor-1 acts through $\alpha 5\beta 1$ integrin. *Blood* **111**, 3479–3488.
- 35 Tan DCW, Manjunatha Kini R, Jois SDS, Lim DKF, Xin L & Ge R (2001) A small peptide derived from Flt-1 (VEGFR-1) functions as an angiogenic inhibitor. *FEBS Lett* **494**, 150–156.
- 36 Lacal PM, Morea V, Ruffini F, Orecchia A, Dorio AS, Failla CM, Soro S, Tentori L, Zambruno G, Graziani G *et al.* (2008) Inhibition of endothelial cell migration and angiogenesis by a vascular endothelial growth factor receptor-1 derived peptide. *Eur J Cancer* **44**, 1914–1921.
- 37 Cianfarani F, Zambruno G, Brogelli L, Sera F, Lacal PM, Pesce M, Capogrossi M, Failla CM, Napolitano M & Odorisio T (2006) Placenta growth factor in diabetic wound healing. *Am J Pathol* **169**, 1167–1182.
- 38 Wiesmann C, Fuh G, Christinger HW, Eigenbrot C, Wells JA & de Vos AM (1997) Crystal structure at 1.7 Å resolution of VEGF in complex with domain 2 of the Flt-1 receptor. *Cell* **91**, 695–704.
- 39 Cao Y, Hoepfner LH, Bach S, E G, Guo Y, Wang E, Wu J, Cowley MJ, Chang DK, Waddell N *et al.* (2013) Neuropilin-2 promotes extravasation and metastasis by interacting with endothelial $\alpha 5$ integrin. *Cancer Res* **73**, 4579–4590.
- 40 Alghamdi AAA, Benwell CJ, Atkinson SJ, Lambert J, Johnson RT & Robinson SD (2020) NRP2 as an emerging angiogenic player; promoting endothelial cell adhesion and migration by regulating recycling of $\alpha 5$ integrin. *Front Cell Dev Biol* **8**, 395.
- 41 Takahashi T, Fournier A, Nakamura F, Wang L-H, Murakami Y, Kalb RG, Fujisawa H & Strittmatter SM (1999) Plexin-neuropilin-1 complexes form functional semaphorin-3A receptors. *Cell* **99**, 59–69.
- 42 Muhl L, Bergsten Folestad E, Gladh H, Wang Y, Moessinger C, Jakobsson L & Eriksson U (2017) Neuropilin-1 binds PDGF-D and is a co-receptor in PDGF-D-PDGFR β signaling. *J Cell Sci* **130**, 1365–1378.
- 43 Robinson SD, Reynolds LE, Kostourou V, Reynolds AR, Gracia da Silva R, Tavora B, Baker M, Marshall JF & Hodivala-Dilke KM (2009) $\alpha v\beta 3$ integrin limits the contribution of neuropilin-1 to vascular endothelial growth factor-induced angiogenesis. *J Biol Chem* **284**, 33966–33981.
- 44 Djordjevic S & Driscoll PC (2013) Targeting VEGF signalling via the neuropilin co-receptor. *Drug Discov Today* **18**, 447–455.
- 45 Graziani G & Lacal PM (2015) Neuropilin-1 as therapeutic target for malignant melanoma. *Front Oncol* **5**, 125.
- 46 Starzec A, Vassy R, Martin A, Lecouvey M, Di Benedetto M, Crépin M & Perret GY (2006) Antiangiogenic and antitumor activities of peptide inhibiting the vascular endothelial growth factor binding to neuropilin-1. *Life Sci* **79**, 2370–2381.

- 47 Jia H, Cheng L, Tickner M, Bagherzadeh A, Selwood D & Zachary I (2010) Neuropilin-1 antagonism in human carcinoma cells inhibits migration and enhances chemosensitivity. *Br J Cancer* **102**, 541–552.
- 48 Pan Q, Chanthery Y, Liang W-C, Stawicki S, Mak J, Rathore N, Tong RK, Kowalski J, Fong Yee S, Pacheco G *et al.* (2007) Blocking neuropilin-1 function has an additive effect with anti-VEGF to inhibit tumor growth. *Cancer Cell* **11**, 53–67.
- 49 Kong J-S, Yoo S-A, Kim J-W, Yang S-P, Chae C-B, Tarallo V, De Falco S, Ryu S-H, Cho C-S & Kim W-U (2010) Anti-neuropilin-1 peptide inhibition of synoviocyte survival, angiogenesis, and experimental arthritis. *Arthritis Rheum* **62**, 179–190.
- 50 Gimbrone MA (1976) Culture of vascular endothelium. *Prog Hemost Thromb* **3**, 1–28.
- 51 Ilari A, Fiorillo A, Poser E, Lalioti VS, Sundell GN, Ivarsson Y, Genovese I & Colotti G (2015) Structural basis of Sorcin-mediated calcium-dependent signal transduction. *Sci Rep* **5**, 16828.
- 52 Cunningham SA, Tran TM, Arrate MP & Brock TA (1999) Characterization of vascular endothelial cell growth factor interactions with the kinase insert domain-containing receptor tyrosine kinase: a real time kinetic study. *J Biol Chem* **274**, 18421–18427.
- 53 Bjellqvist B, Hughes GJ, Pasquali CH, Paquet N, Ravier F, Sanchez J-C, Frutiger S & Hochstrasser DF (1993) The focusing positions of polypeptides in immobilized pH gradients can be predicted from their amino acid sequences. *Electrophoresis* **14**, 1023–1031.
- 54 Berman HM, Westbrook J, Feng Z, Gilliland G, Bhat TN, Weissig H, Shindyalov IN & Bourne PE (2000) The Protein Data Bank. *Nucleic Acids Res* **28**, 235–242.
- 55 Guex N & Peitsch MC (1997) SWISS-MODEL and the Swiss-PdbViewer: an environment for comparative protein modeling. *Electrophoresis* **18**, 2714–2723.